Knowles, J. R. (1987) *Science 236*, 1252–1258.
Knox, J. R., & Moews, P. C. (1991) *J. Mol. Biol. 220*, 435–455.
Kunkel, T. A. (1985) *Proc. Natl. Acad. Sci. U.S.A. 82*, 488–492.
L'Enfant, F., Labia, R., & Masson, J. M. (1991) *J. Biol. Chem. 266*, 17187–17194.
Moews, P. C., Knox, J. R., Dideberg, O., Charlier, P., & Frère, J. M. (1990) *Proteins: Struct., Funct., Genet. 7*, 156–171.
Olovsson, I., & Jönsson, P. G. (1976) in *The Hydrogen Bond* (Schuster, P., Zundel, G., & Sandorfy, C., Eds.) Vol. 2, pp 393–456, North-Holland, Amsterdam.
Sanger, F., Milken, S., & Coulson, A. R. (1977) *Proc. Natl. Acad. Sci. U.S.A. 74*, 5463–5467.
Schwinghamer, E. A. (1980) *FEMS Microbiol. Lett. 7*, 157–162.
Virden, R., Tan, A. K., & Fink, A. L. (1990) *Biochemistry 29*, 145–153.

Conformational Similarities between One-Chain and Two-Chain Tissue Plasminogen Activator (t-PA): Implications to the Activation Mechanism on One-Chain t-PA†

Vicki L. Nienaber,‡,§ Sharon L. Young,‖ Jens J. Birktoft,*,⊥ Deborah L. Higgins,‖,# and Lawrence J. Berliner*,‡

Department of Chemistry, The Ohio State University, Columbus, Ohio 43210, Department of Biochemistry and Molecular Biophysics, Washington University School of Medicine, St. Louis, Missouri 63110, and Department of Cardiovascular Research, Genentech, Inc., South San Francisco, California 94080

Received April 12, 1991; Revised Manuscript Received January 30, 1992

ABSTRACT: Tissue plasminogen activator (t-PA) is an exceptional serine protease, because unlike most other serine protease zymogens single-chain tissue plasminogen activator (sct-PA) possesses a substantial amount of proteolytic activity. The unusual reaction of sct-PA afforded the opportunity to directly compare the active site environment of sct-PA and two-chain tissue plasminogen activator (tct-PA) in solution through the application of a series of nitroxide spin labels and fluorophores. These labels, which have been previously shown to covalently label the catalytic serine of other serine proteases, inactivated both sct-PA and tct-PA. The labels can be divided into two classes: those which form tetrahedral complexes (sulfonates) and those which form trigonal complexes (anthranilates). Those which formed tetrahedral complexes were found to be insensitive to structural differences between sct-PA and tct-PA at the active site. In contrast, those which formed trigonal complexes could differentiate and monitor the sct-PA to tct-PA conversion by fluorescence spectroscopy. Models of the structure of sct-PA and tct-PA were constructed on the basis of the known X-ray structures of other serine protease zymogen and active enzyme forms. One of the nitroxide spin labels was modeled into the sct-PA and tct-PA structures in two possible orientations, both of which could be sensitive to structural differences between sct-PA and tct-PA. These models formed the structural rationale used to explain the results obtained with the "tetrahedral" and "trigonal" probes, as well as to offer a possible explanation for the unique reactivity of sct-PA.

The enzymes of the mammalian serine protease family, i.e., trypsin, chymotrypsin, and elastase, are highly homologous in structure and catalytic mechanism. In addition, most of these enzymes are biosynthesized as a single-chain proenzyme or zymogen which is almost entirely devoid of enzymatic activity. The inactive zymogen form of all of these proteins requires activation via limited proteolysis in order to yield significant amounts of enzyme activity. The activation of trypsinogen and chymotrypsinogen results in an amplification of activity which has been estimated to be around 10^7–10^8 (Kerr et al., 1975).

Tissue plasminogen activator (t-PA)[1] is an atypical serine protease because the zymogen form, sct-PA, has significant enzymatic activity. This has been most clearly shown by the analysis of variants of t-PA in which the arginyl residue at

† This work was supported in part by a grant from the National Heart Lung and Blood Institute (HL 24549) to L.J.B. and from the Lucille P. Markey Charitable Trust for Research in Molecular Biology and Human Disease at the Washington University School of Medicine to J.J.B.

‡ The Ohio State University.
§ Current address: Department of Biochemistry and Molecular Biophysics, Washington University School of Medicine, St. Louis, MO 63110.
‖ Genentech, Inc.
⊥ Washington University School of Medicine.
Current address: RiboGene, 21375 Cabot Blvd., Hayward, CA 94545.

[1] Abbreviations: t-PA, tissue plasminogen activator; tct-PA, two-chain tissue plasminogen activator; sct-PA, single-chain tissue plasminogen activator; S-2288, H-D-Ile-Pro-Arg-nitroanilide; BPTI, bovine pancreatic trypsin inhibitor; PSTI, pancreatic secretory trypsin inhibitor; DFP, diisopropyl fluorophosphate; ESR, electron spin resonance; *p*-V (*p*-CO-5NH), 4-(2,2,5,5-tetramethylpyrrolidine-1-oxyl)-*p*-(fluorosulfonyl)-benzamide; *m*-IV (*m*-CO-6NH), 4-(2,2,6,6-tetramethylpiperidine-1-oxyl)-*m*-(fluorosulfonyl)benzamide; *m*-V (*m*-CO-5NH), 3-(2,2,5,5-tetramethylpyrrolidine-1-oxyl)-*m*-(fluorosulfonyl)benzamide; *m*-VII (*m*-NCO-6NH), *N*-[*m*-(fluorosulfonyl)phenyl]-4-*N*-(2,2,6,6-tetramethylpiperidine-1-oxyl)urea; R275E-sct-PA, single-chain t-PA in which Arg 275 has been replaced by glutamate; S-2251, H-D-Val-Leu-Lys-*p*-nitroanilide; MMTS, methyl methanethiolsulfonate.

0006-2960/92/0431-3852$03.00/0

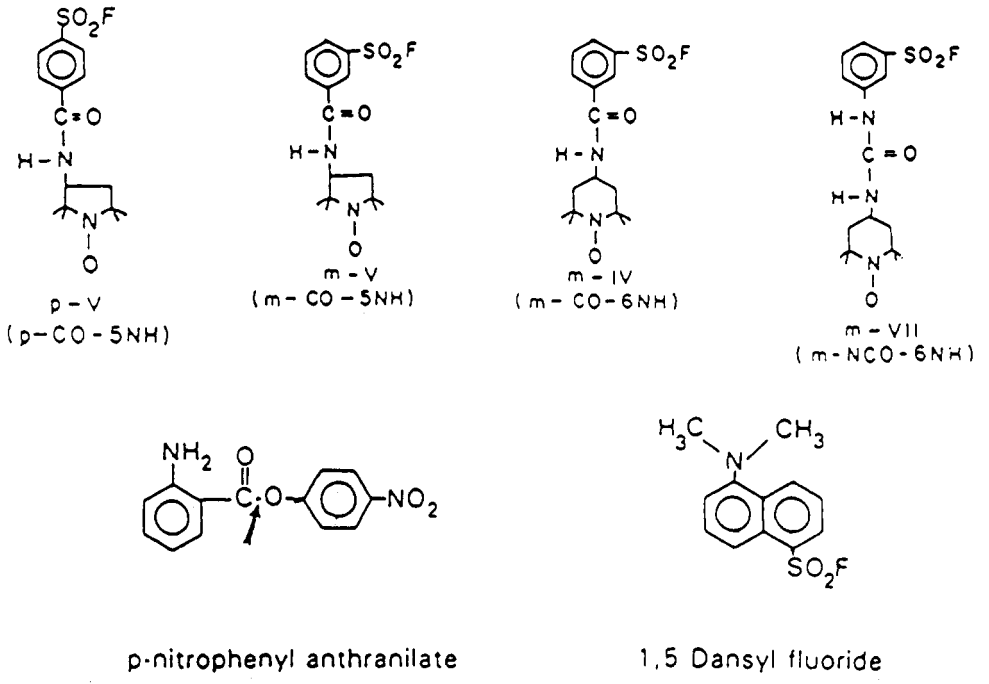

FIGURE 1: Structures of the nitroxide spin labels and fluorophores used in this study.

the "activation" site, position 275, was replaced with a nonbasic residue making the molecule resistant to plasmin activation to the two-chain form (Tate et al., 1987; Petersen et al., 1988; Boose et al., 1989). These groups found that in the presence of the physiological stimulators related to fibrin and the physiological substrate, plasminogen, the activity of sct-PA and tct-PA was similar. With low molecular weight substrates, the conversion of sct-PA to tct-PA was accompanied by an increase in rate of plasminogen activation of only about 3–6-fold (Tate et al., 1987; Boose et al., 1989). In another study employing the synthetic substrate S-2288, Urano et al. (1989) were able to directly measure the amidolytic activity of t-PA and found that the activity of sct-PA was enhanced in the presence of fibrinogen to the extent that its activity was equal to that of tct-PA. Loscalzo (1988) found that the activity of both sct-PA and tct-PA toward S-2288 was enhanced in the presence of fibrin monomers.

X-ray crystallographic studies of the zymogen–enzyme pairs trypsinogen–trypsin and chymotrypsinogen–chymotrypsin indicate that the structure of each zymogen and its corresponding enzyme form are largely identical. The only region of significant structural differences is located at the newly generated α-amino terminus, Ile 16 (Ile 276),[2] and at residues 189–194 (472–477), which constitute part of the substrate-binding pocket (Freer et al., 1970; Huber & Bode, 1978). In addition, trypsinogen complexes with the proteinase inhibitor, BPTI or PSTI, as well as DFP inactivation of this zymogen result in a conformational change into an "active" conformation nearly identical to that of trypsin (Bode, 1979; Bolognesi et al., 1982; Jones & Stroud, 1986).

Nitroxide spin labels and fluorophores, such as those employed in this study (Figure 1), have been demonstrated to be effective and sensitive probes for monitoring small changes in protein structure in solution. In particular, the active site conformations of several serine proteases have been compared to great detail using fluorosulfonyl phenyl nitroxide spin labels (Berliner & Wong, 1974; Berliner et al., 1981). Specifically, these labels have been able to sense conformational differences between the α and γ forms of human thrombin (Berliner et al., 1981), as well as the human and bovine forms of thrombin (Neinaber & Berliner, 1991). The high reactivity of sct-PA afforded the opportunity to incorporate active site directed spin labels and fluorescent probes into both sct-PA and tct-PA, allowing a direct comparison of the active site environment of these two enzyme forms. Molecular models of the protease domains of sct-PA and tct-PA were employed to further analyze the results of this study.

Materials and Methods

Proteins. tct-PA was prepared from Activase alteplase by the method of Higgins and Vehar (1987). The R275E sct-PA mutant was prepared by the procedure of Tate et al. (1987). Protease (*Staphylococcus aureus*) V8 was from ICN Biochemicals. R275E sct-PA was converted into a form of tct-PA analogous to wild-type tct-PA by protease (*S. aureus*) V8 as described (Tate et al., 1987). R275E sct-PA and R275E tct-PA have been shown to have properties similar to those of the corresponding wild-type forms (Tate et al., 1987). Fibrinogen was from Miles Diagnostics. Plasmic fragments were prepared by incubating fibrinogen with plasmin-Sepharose overnight at 37 °C. The clotability of the resulting product was <10%.

Chemicals. The fluorosulfonyl spin labels were synthesized by the method of Wong et al. (1974). The chromogenic tripeptide substrates H-D-Val-Leu-Lys-*p*-nitroanilide (S-2251) and H-D-Ile-Pro-Arg-*p*-nitroanilide (S-2288) were from Helena Laboratories. Dansyl fluoride and *p*-nitrophenyl anthranilate were from Molecular Probes. Methyl methanethiosulfonate (MMTS) was purchased from Aldrich Chemical Co. Tris-HCl and arginine-HCl were from Sigma Chemical Co. Sodium phosphate, monobasic and dibasic, were from Mallinckrodt and Baker Chemicals, respectively. Tween 80

[2] The primary numbering system employed is based on bovine chymotrypsinogen A (Hartley, 1970), while that based on t-PA is given in parentheses.

(polysorbate 80) was obtained from Emulsion Engineering, Inc. Acetonitrile and 2-propanol were from Fisher Scientific and Mallinckrodt, respectively.

ESR. tct-PA was labeled with a 10-fold molar excess of nitroxide spin label relative to the protein concentration, which was typically 2–5 mg/mL. The reaction was allowed to proceed 1–3 h in 0.08M phosphate, 0.17 M arginine-HCl, 0.0008% tween 80, and 10% (v/v) acetonitrile cosolvent after which 60–90% of the protein was labeled as determined by loss of S-2251 or S-2288 activity. Unreacted label was removed by exhaustive dialysis against the reaction buffer.

R275E-sct-PA was labeled by the same procedure as tct-PA with the following modification. Some of the fluorosulfonyl spin labels tested were found to react at Cys 83, in addition to the active site serine (V. L. Nienaber and L. J. Berliner, unpublished results). To overcome this, the enzyme was first labeled at Cys 83 with a 200-fold molar excess of MMTS for 12–18 h, followed by the spin labeling procedure used for tct-PA.

ESR spectra were recorded at 20 ± 2 °C on a Varian E-4 spectrometer in quartz flat cells with a Varian E-257 variable temperature accessory. Typical instrument conditions were microwave frequency, 9.15 GHz; microwave power, 20 mW; modulation frequency, 100 MHz; applied field, 3256 G; scan range, 100 G; modulation amplitude, 2.0 G. Measurements of the maximal separation in hyperfine extrema, $2T_{\parallel}$, were taken from "high gain" spectra measured immediately after obtaining low gain spectra. High gain spectra were typically run at 4–10-fold higher receiver gain and 1–4-fold higher modulation amplitude to enhance these peaks.

Protein concentrations were estimated spectrophotometrically on a Kontron Uvikon 860 using an ϵ_{280} = 1.9 mL g^{-1} cm^{-1} for both enzymatic forms and a M_r value of 59 000.

Fluorescence. The incorporation of dansyl fluoride into t-PA was carried out in a cosolvent of 2-propanol (5–10% v/v) and was allowed to proceed 20–24 h at room temperature after which 60–80% of the protein was labeled by S-2288 activity assays. The *p*-nitrophenyl anthranilate reaction was allowed to proceed 24 h at room temperature after which 40–50% of the protein was labeled.

Fluorescence spectra were recorded on a Perkin Elmer MPF-44 fluorescence spectrometer at 25 ± 1 °C.

Model Building of t-PA Models. Protein coordinates were obtained from the Brookhaven Protein Data Bank (Bernstein et al., 1977). The model construction and analysis was conducted on Silicon Graphics 4D IRIS workstations using the program packages TOM (Cambillau et al., 1987) and TURBO-FRODO (Roussel and Cambillau, personal communication). Molecular dynamics and energy "refinement" calculations were performed on the IRIS workstations using the XPLOR program package (Brunger, 1988). Amino acid sequences were extracted from the Protein Identification Resource data base using the Wisconsin CGC program package (Devereux et al., 1984). This program package was also used for the alignment and manipulations of amino acid sequences.

Analysis of an amino acid sequence alignment for the mammalian serine proteases, which previously had been developed for studies of thrombin (Sugawara et al., 1986; Berliner et al., 1987) and coagulation factor IXa (Bajaj et al., 1989), suggested that the three-dimensional structure of chymotrypsin would form the best basis for the comparative model building of the protease domains of the one- and two-chain forms of t-PA. Although the specificity of t-PA resembles that of trypsin, chymotrypsin was chosen as the starting point because the distribution of disulfide bridges in t-PA is more similar to that seen in chymotrypsin and fewer insertions are necessary to align the sequences. The current sequence alignment incorporates the amino acid sequences of some 20 different proteases. The guiding principle, in the modeling, was based on the structural homology among the serine proteases as established via X-ray diffraction analysis of chymotrypsin (Birktoft & Blow, 1972), elastase (Sawyer et al., 1978), and trypsin (Stroud et al., 1974; Bode et al., 1978) and later extended with structure determinations of tonin (Fujinaga & James, 1987), kallikrein (Chen & Bode, 1983), rat mast cell protease (Remington et al., 1988), and neutrophil elastase (Navia et al., 1989).

For the construction of the structures of the protease domains of tct-PA and of sct-PA in the so-called "active conformation", subunit B of α-chymotrypsin [BNL-PDB code 5CHA (Blevins & Tulinsky, 1985)] was used as the starting framework, while subunit B of chymotrypsinogen [BNL-PDB code 2CGA (Wang et al., 1985)] was used for sct-PA in the so-called "zymogen conformation". The complexes of trypsinogen with secretory trypsin inhibitor [BNL-PDB code 1TGS (Bolognesi et al., 1982)] and of trypsin with pancreatic trypsin inhibitor [BNL-PDB code 4TPI (Bode et al., 1984)] were used in guiding the construction of models for complexes of sct-PA and tct-PA with substrates and inhibitors, respectively. Except for the few regions of insertion/deletions, the conformation of the polypeptide main chain of the starting model was left unchanged. The side chains in chymotrypsin and chymotrypsinogen were replaced with the requisite residues to create t-PA using the program DELPHI (Kimmel, 1987). This program permits the replacement of amino acid side chains and subsequent adjustment by rotation around side-chain bonds in order to eliminate or minimize improper stereochemistry. The guiding principle was, in general, that when the amino acid residue in t-PA is identical to that in a serine protease of known structure, the side-chain conformation in that protease's structure was used as a template for the t-PA model. For internal residues that contain polar atoms, an attempt was made to orient the polar atoms in such a way that it could participate in a hydrogen bond. In the serine proteases, such hydrogen bonds frequently involve solvent molecules that are located at internal positions (Birktoft & Blow, 1972). Trypsin, elastase, and the other protease crystal structures contain solvent molecules in homologous positions, and at least half of these are conserved in all the serine enzymes (Birktoft, unpublished). These internal waters have also been conserved in the putative t-PA structures, but it should be emphasized that no solvent molecules have been introduced that do not have a counterpart in a protease structure of known structure. The enzymatic specificity of t-PA most closely resembles that of trypsin. In the substrate-binding region of known serine protease structures, the amino acid sequence of t-PA most closely resembles that of trypsin and kallikrein and less so that of chymotrypsin. In this region, the substrate-binding site, the t-PA structure was adjusted to match most closely that of trypsin.

At eight locations, the length of the t-PA polypeptide chain differs from that of chymotrypsin. Such differences can all be located on the surface of the protease domain, in agreement with proposals regarding the general location of deletions and insertions [see, for example, Craik et al. (1983)]. Relative to bovine α-chymotrypsin, a single deletion of one residue is observed while insertions are observed at seven different points in the sequence. Where the length of the polypeptide chain of the t-PA differs from that of chymotrypsin but matches that of a different protease structure, the fragment fitting method

of Jones and Thirup (1986) was used. A library of the seven known serine protease structures provided the latter data base for this purpose. Since the serine proteases are predominantly composed of antiparallel β-sheet structures, an additional data base was formed from all known crystal structures where this form of secondary structure is prevailing. The latter data base proved to be particularly useful in modeling unique insertion loops, where the length of the polypeptide chain did not have a counterpart in any other protease structure. In two instances, the insertions have no counterpart in any other known serine protease structure, and these were modeled as extended loops. One of these insertions, between residues 111 (380) and 112 (385), contains a cysteine residue that is part of a S–S bridge, Cys 50 (315)–Cys 111D (384), observed only in t-PA and urokinase. The disulfide bridge appears to be located on the surface and can be accommodated without difficulty into the chymotrypsin and chymotrypsinogen framework. The longest unique insertion in t-PA relative to chymotrypsin is eight additional residues located between 184 (459) and 187 (470). This insertion is located in a loop between two β-strands and extends toward the molecular surface. In thrombin this loop contains three fewer residues than t-PA while other proteases, including all those for which structural coordinates are available, have six or eight residues fewer than t-PA. A less obvious model for this insertion can be proposed, and for the proposed t-PA models this is the least reliable region.

Areas of unreasonable stereochemistry consisting mainly of close nonbonded contacts were identified by passing the resulting models through an energy minimization and simulated annealing "refinement" using the program XPLOR. Those internal water molecules that were deemed to be part of the t-PA structures were included in the "energy refinement". Errors in stereochemistry and nonbonded interactions were corrected using manual intervention on the graphics system, and the resulting models were further checked via XPLOR calculations. It should be emphasized that these final t-PA models have been subjected only to a minimum of computational adjustments and that these adjustments have affected only the positions of residues in regions of insertions and deletions. The conclusions drawn in this work have been drawn with constant attention to the fact that insertion regions are extremely difficult to model. Furthermore, none of the conclusions are dependent on the fine details of these putative t-PA models.

Results

Labeling Kinetics. The sulfonyl fluoride group of the nitroxide spin labels and fluorophores employed in these studies has been shown to react at the active site serine in a number of the serine proteases (Berliner & Wong, 1974; Berliner & Shen, 1977a,b; Vaz & Schoellmann, 1976). Similarly, the catalytic serine 195 (478) of t-PA was found to react with these labels, resulting in a decrease in t-PA S-2288 activity. R275E t-PA was used in these studies rather than wild-type t-PA due to the difficulty in obtaining wild-type t-PA which is completely in the one-chain form. Previous studies (Tate et al., 1987) have shown that R275E t-PA behaves as one would expect sct-PA to behave. Both tct-PA and R275E t-PA with or without pretreatment with MMTS were inhibited by the nitroxide spin labels and fluorophore tested.

ESR. Figure 2 shows that the ESR spectra of *m*-IV R275E-sct-PA and tct-PA have similar line shapes. A quantitative comparison of these two spectra may be made by correlating the maximum hyperfine splitting, $2T_{\parallel}$ (indicated by arrows), as this parameter is directly related to the motion of the nitroxide moiety. *m*-IV R275E-sct-PA and tct-PA were

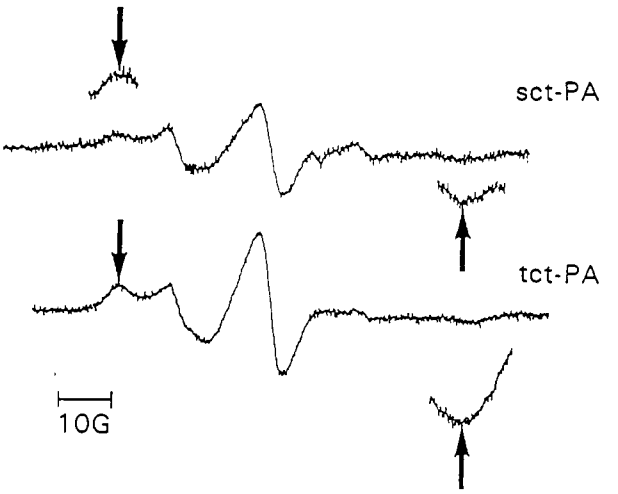

FIGURE 2: X-band ESR spectra of *m*-IV-labeled MMTS R275E-sct-PA and tct-PA. Conditions were 0.08 M sodium phosphate, 0.17 M arginine hydrochloride, and 0.008% Tween 80, pH 7.2, at 20 °C.

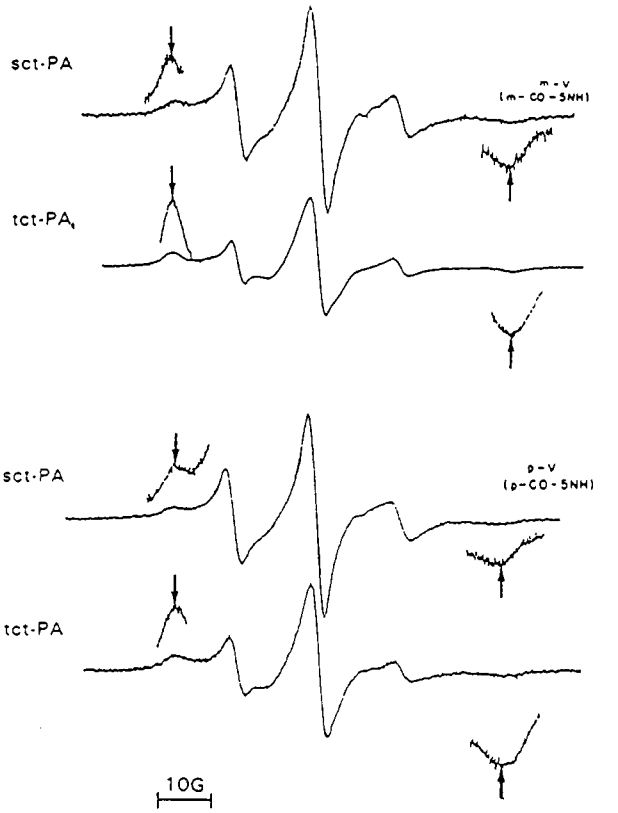

FIGURE 3: X-band ESR spectra for active site labeled *m*-V MMTS R275E-sct-PA, *m*-V tct-PA, *p*-V MMTS R275E-sct-PA, and *p*-V tct-PA. Conditions were as in Figure 1.

found to give rise to identical $2T_{\parallel}$[3] (63.6 G R275E-sct-PA; 63.4 G tct-PA), indicating that the active site environments of R275E-sct-PA and tct-PA are very similar. Figure 3 shows ESR spectra for R275E-sct-PA and tct-PA labeled with the meta- and para-substituted spin labels *m*-V and *p*-V, respectively.[4] The spectra suggest that *m*-V is interacting with

[3] $2T_{\parallel}$ are correct to ±0.5 G.

[4] The minor sharp components of these spectra are due to spin label reaction at presumably unblocked Cys 83. For R275E-sct-PA, these components were much more pronounced for samples which were not first treated with MMTS.

Table I: Relative Fluorescence Emission of Anthraniloyl-t-PA Form

protein	I_{ex} (287 nm)[a]	I_{ex} (350 nm)[b]	I (287)/ I (350)	I_{em} (416 nm)[d]
R275E-sct-PA	100%	100%	0.93	100%
tct-PA	58.5%	49.0%	1.12	54%

[a] Relative intensity of the 287-nm excitation band, monitored at 416 nm. [b] Relative intensity of the 350-nm excitation band, monitored at 416 nm. [c] Ratio of the absolute intensities of the 287- and 350-nm excitation bands, monitored at λ_{em} = 416 nm. [d] Relative intensity of the fluorescence emission at 416 nm; λ_{ex} = 350 nm.

R275E-sct-PA and tct-PA in a manner unlike *m*-IV by virtue of the differences in line shape and $2T_{\parallel}$ values (see Figure 2). Inspection of the spectra in Figure 3A,B shows that *m*-V did not sense a structural difference between R275E-sct-PA and tct-PA (*m*-V R275E-sct-PA, $2T_{\parallel}$ = 66.5 G; *m*-V tct-PA, $2T_{\parallel}$ = 66.6 G). Similarly, results obtained with the para-substituted analogue *p*-V differed in $2T_{\parallel}$ from those of *m*-V but suggested as well that the active site environment of the two enzyme forms was similar (R275E-sct-PA, $2T_{\parallel}$ = 63.2 G; tct-PA, $2T_{\parallel}$ = 63.5 G).

In the case of *m*-VII, it was difficult to measure accurate $2T_{\parallel}$ values since the nitroxide was only moderately immobilized. In this case, the splitting from the center field to the high field line of the ESR spectrum was measured and found to be 31.0 G for both R275E-sct-PA and tct-PA (data not shown). Thus, again here the spin label spectra indicated identical extended active site environments in both forms of t-PA.

In order to probe fibrin binding interactions, equimolar concentrations of fibrinogen or plasmin degraded fibrinogen fragments were added to spin-labeled R275E-sct-PA and tct-PA. None of these additions effected the spectra of any of the spin-labeled t-PA derivatives under these conditions (data not shown).

Fluorescence. R275E-sct-PA and tct-PA were labeled with the active site directed fluorophores 1,5-dansyl fluoride and *p*-nitrophenyl anthranilate (Figure 1). As observed in the ESR studies, the excitation and emission spectra of dansyl R275E-sct-PA and tct-PA were found to be identical (identical excitation, emission maxima, and quantum yield).[5] Similar to dansyl binding to other serine proteases, the dansyl-t-PA excitation spectrum (λ_{em}^{max} = 516 nm) consisted of two bands at 289 and 360 nm (Berliner & Shen, 1977b; Vaz & Schoellmann, 1976). The band at 360 nm was due to the label emission, while the band at 289 nm corresponded to energy transfer originating from one or more tryptophans on the protein.

In contrast to the results obtained with the fluorosulfonyl labels, *p*-nitrophenylanthranilate was unique in that it did detect differences between R275E-sct-PA and tct-PA. Figure 4A shows that anthraniloyl-R275E-sct-PA and -tct-PA gave rise to identical emission maxima. However, the quantum yield of R275E-sct-PA was approximately twice that of tct-PA. In fact, it was possible to monitor the V8 protease catalyzed R275E-sct-PA to tct-PA conversion via changes in the anthraniloyl fluorescence (Figure 4B), which paralleled the change in the S-2288 hydrolysis rate (data not shown). The conversion was also confirmed by SDS–PAGE (data not shown). In addition, as listed in Table I, the ratio of the energy transfer peak to the label emission peak (I_{287}/I_{350}) was larger for anthraniloyl-tct-PA relative to -sct-PA. This result again indicated that the anthraniloyl moiety was interacting with

[5] Wavelength maxima are accurate to ±0.5 nm.

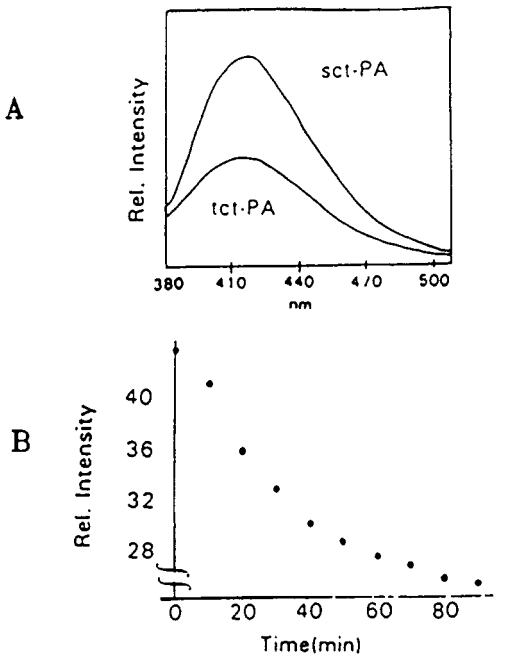

FIGURE 4: (A) Fluorescence emission spectra of anthraniloyl R275E-sct-PA and tct-PA (V8 protease conversion product of R275E-sct-PA). (B) Proteolytic conversion of anthraniloyl-R275E-sct-PA into tct-PA by V8 protease as monitored by anthraniloyl fluorescence. Conditions were 40 mM Tris-HCl, pH 7.2, 25 °C, λ_{ex} = 350 nm.

R275E-sct-PA and tct-PA differently which could signify that the primary intrinsic energy transfer donor [possibly Trp 215 (498)] of t-PA was closer to the anthraniloyl moiety on tct-PA relative to R275E-sct-PA.

Finally, fibrinogen was added to both forms of anthraniloyl-t-PA. While addition of fibrinogen (5 μM) was found to have no effect on the fluorescence of anthraniloyl-tct-PA, a quenching of about 10% of the fluorescence of anthraniloyl-R275E-sct-PA was observed (data not shown). The change in intensity upon the addition of fibrinogen was in the same direction as that observed for the conversion of R275E-sct-PA to tct-PA.

Structural Implications from Molecular Modeling. Overall, the putative models of the sct-PA and tct-PA protease domains were constructed without any significant problems. Indications of the general correctness of the putative structure(s) were provided by the observations that (1) no charged amino acids were introduced into internal locations remote from the solvent; and (2) the disulfide Cys 50 (315)–Cys 111D (484) bridge unique for t-PA could be easily adapted into the structure. The only region that created slight difficulties was the eight-residue insertion between residues 184 (459) and 187 (470) relative to chymotrypsin (a six-residue insertion relative to trypsin). As noted earlier, this eight-residue insertion is unique to t-PA and is not observed in any other known serine protease sequence. The only other serine protease that has an insertion at this position is thrombin where the insertion is five residues longer relative to chymotrypsin.

The starting models for the two forms of t-PA were chymotrypsinogen (sct-PA) and chymotrypsin (tct-PA), although the corresponding trypsinogen/trypsin pair could have been applied as well. The overall sequence homology between t-PA and trypsin or chymotrypsin is about 44% and 40%, respectively, using the sequence alignment specifications noted under Materials and Methods. Furthermore, none of the conclusions presented here are very dependent upon the choice of starting model.

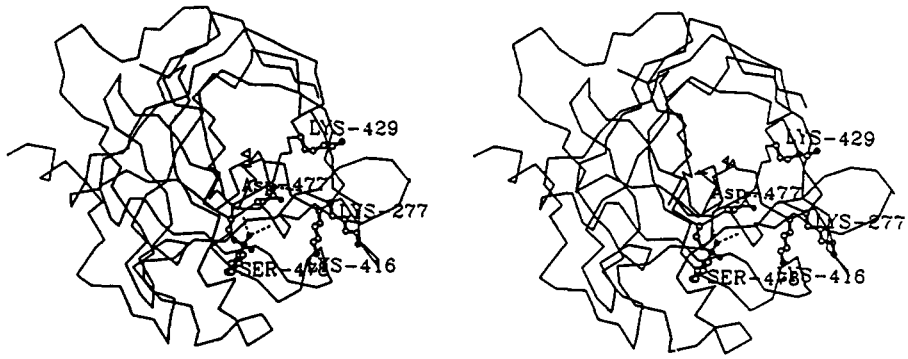

FIGURE 5: Putative molecular models of the protease domains of tct-PA. The stereodiagrams show α-carbon models of the protease domains of tct-PA complexed with a nitroxide spin label. The side chains of lysine residues 17 (277), 143 (416), and 156 (429) and of Asp 194 (477) are shown as ball and stick models. A spin label is shown attached to the hydroxyl group of the catalytic Ser 195 (478); however, for the sake of clarity only the sulfonyl–phenyl part of the spin label has been included, while the nitroxide part has been omitted. Hydrogen bonds between the carboxyl group of Asp 194 (477) and the free α-amino group of Ile 16 (176) and between one of the sulfonyl oxygens and the main-chain amido nitrogens of Gly 193 (476) and Ser 195 (478) in the oxyanion hole are shown as stippled lines. The only significant differences between this model of the tct-PA structure and the "active conformation" of sct-PA are in the vicinity of the activation cleavage site, Arg 15 (275)–Ile 16 (276) and near Asp 194 (477).

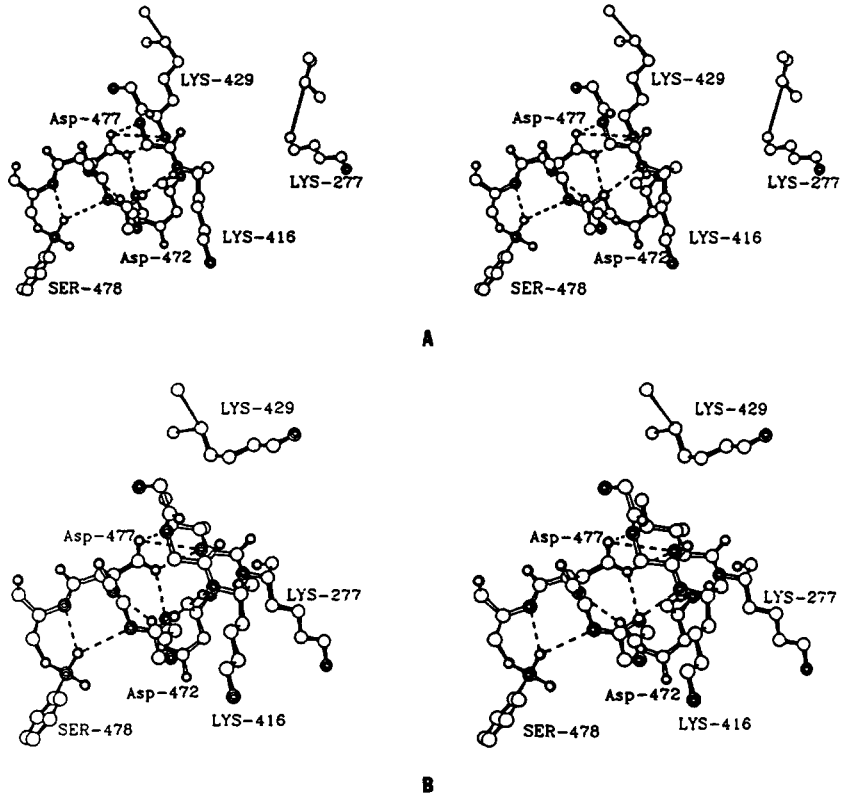

FIGURE 6: Closeup of the environment of Asp 194 (477) in sct-PA and tct-PA. The views is the same as that used in Figure 5. (A) Stereodiagram of sct-PA. Included are the α-carbon atoms of residues 16–17 (276–277), 155–157 (428–430), the main-chain atoms of residues 189 (472), 140–143 (411–416), and 474–478 (191–195) as well as the side chains of Ile 16 (276), Lys 17 (277), Lys 143 (416), Lys 156 (429), Asp 189 (472), Asp 194 (477), and Ser 195 (478) with part of a nitroxide spin label covalently attached to the O^{γ} hydroxyl. Only the phenylsulfonyl moiety of the spin label is shown. The carboxylate of Asp 194 (477) is stabilized by interactions with the amino group of Lys 156 (429) and by hydrogen bonds to the NH of Gly 142 (415) and Cys 191 (474). One of the two sulfonyl oxygens is stabilized by hydrogen bonds to the oxyanion hole. These hydrogen bonds are all shown as thick stippled lines. (B) Stereodiagram of tct-PA. The included residues and their representation are as in panel A. In tct-PA the carboxylate of Asp 194 (477) is stabilized by interactions with the amino group of Ile 16 (276) and by hydrogen bonds to the NH of Gly 142 (415) and Cys 191 (474), shown as stippled lines. Notice that the major differences between sct-PA and tct-PA are the location and interactions of residues 16 (276) and 17 (277).

Figure 5 shows an α-carbon model of the putative protease domain of tct-PA. Also included in this figure are the side chains of lysine residues 277, 416, and 429 and of Asp 477. A spin label is shown attached to the hydroxyl group of the catalytic Ser 195 (478); however, for the sake of clarity only the sulfonyl–phenyl part of the spin label has been included, while the nitroxide part has been omitted. Figure 6A,B presents close up views of the active site region of sct-PA and tct-PA, respectively, shown in the same orientation used in Figure 5, and with the sulfonyl group covalently attached to the hydroxyl group of the catalytic Ser 195 (478). In these models, one of the sulfonyl oxygens is interacting at the oxyanion hole [i.e., hydrogen bonded to main-chain amido nitrogens of Gly 193 (476) and Ser 195 (478); see also Figure 6], in the *same manner* observed for other sulfonyl complexes with α- and γ-chymotrypsin, trypsin, elastase, and subtilisins (Kraut, 1977). Thus, depending on which one of the two sulfonyl oxygens is placed in the oxyanion hole, the spin-label can be placed in one or two locations. Using the same convention applied to the description of other spin-labeled serine

proteases (Berliner et al., 1987), the two orientations are named "up" and "down". The orientation shown in Figures 5 and 6 corresponds to the down position.

In the "down position" the spin label is located in the general vicinity of the substrate-binding site with the phenyl ring of the label located at the mouth of the substrate-binding pocket which includes residues Met 192 (475), Ser 214 (497), Trp 215 (498), and Gly 216 (499). The positioning and mobility of the spin label would be affected by the binding of specific inhibitors in the substrate pocket. This was observed previously for indole or dioxane binding to chymotrypsin (Berliner & Wong, 1974) and was also observed with benzamidine binding to t-PA (V. L. Nienaber and L. J. Berliner, unpublished results). In the "up position" two regions seem accessible to the nitroxide group. One region is near residues Cys 58 (323), Phe 59 (324), and Glu 60 (325), and the other is near residues Ile 33 (293)–Leu 41 (306).

The conformational shift occurring during the "zymogen" to "active enzyme" transition significantly alters the location of Gly 193 (476); in fact, in the *zymogen conformation* the oxyanion hole is incomplete and would be incapable of providing stabilization (Freer et al., 1970; Birktoft et al., 1976; Huber & Bode, 1978). Thus, this conformational shift would result in a dramatic change in the spin label environment and the corresponding ESR spectrum whether the spin label is in the *up or down* position. Furthermore, when in the down position, interactions of other parts of the spin label (i.e., the aromatic ring, the NHCO link and the heterocyclic nitroxide ring) with the t-PA substrate binding site should be altered during the sct-PA to tct-PA transition.

As alluded to previously, stabilization of Asp 194 (477) by the newly formed α-amino group of Ile 16 (276) is a key driving force in the formation of the active (two-chain) enzyme conformation. In Figure 6A,B, close-up models of the environment of Asp 194 (477) in sct-PA and tct-PA are shown. In tct-PA (Figure 6B) Asp 194 (477) is stabilized by the α-amino group of Ile 16 (276), as observed for other serine proteases. The environment of Asp 194 (477) in the "active conformation" of sct-PA is shown in Figure 6A.

Although in this model Ile 16 (276) is incapable of stabilizing Asp 194 (477), three lysine residues, at positions 16 (277), 143 (416), and 156 (429), could assist in this stabilization. On the basis of this model, Lys 156 (429) appears to be the most likely candidate for stabilizing Asp 194 (477) in sct-PA. Figure 6A shows that Lys 16 (277) is most likely too far from Asp 194 (477) to contribute to sct-PA stabilization while Lys 143 (416) is pointing out into solution and away from Asp 194 (477). However, since these observations are based on models rather than the actual t-PA structures, it is impossible on this basis to rule out contributions from Lys 16 (277) and Lys 143 (416).

Discussion

The active site environments of R275E-sc-PA and tct-PA were compared through the use of a number of nitroxide spin labels and fluorophores. All fluorosulfonyl labels tested reported that the active site environments of R275E-sct-PA and tct-PA were very similar, if not identical. In fact, the only label capable of distinguishing R275E-sct-PA and tct-PA was *p*-nitrophenyl anthranilate, which forms a stable trigonal complex with Ser 195 (478) of this enzyme. The results of these studies will be discussed in two parts: results with fluorosulfonyl labels and results with the acyl label, *p*-nitrophenylanthranilate.

It is remarkable that the fluorosulfonyl labels interact in essentially identical manners at the active site of R275E-sct-PA and tct-PA when one considers that these two forms of t-PA display different catalytic rates for both plasminogen activation (in the absence of a fibrin related stimulator) and S-2288 hydrolysis. Previously, these fluorosulfonyl labels have been shown to be sensitive to subtle conformational differences between the α and γ forms of human thrombin (Berliner et al., 1981) as well as to conformational changes propagated to the active site of thrombin upon binding biological effectors such as thrombomodulin (Musci et al., 1988). Since each spin label has a different molecular geometry and gave rise to a unique $2T_{\parallel}$, it is clear that each probed a slightly different area of the active site of R275E-sct-PA and tct-PA. In another study, Higgins and Lamb (1986) studied a dansyl tripeptide–chloromethylketone inhibited form of R275E-sct-PA and tct-PA and found that the environment of this fluorescent probe was the same for both forms of t-PA. This dansyl tripeptide is expected to bind in a normal substrate orientation but to monitor an area different from that of the fluorosulfonyl labels. This study supports the results reported here which suggest that *when a substrate or substrate analogue is bound*, the active site of sct-PA is essentially identical to that of tct-PA.

Previous X-ray crystallographic studies have demonstrated that it is possible to generate a functional structure of serine protease zymogen without cleavage of the Lys/Arg–Ile/Val peptide bond (Bolognesi et al., 1982). Thus, this cleavage is not essential for the generation of an active enzyme for some serine proteases. One example is the mature form of the fungal enzyme, α-lytic protease, which has an additional dipeptide located at the amino terminus that is not cleaved. However, this enzyme retains a normal active enzyme conformation because the side chain of Arg 138 provides the counterion for the Asp 194 (477) carboxylate which is normally provided by the free α-amino group of residue 16 in other proteases. Consequently, the conformation of residues 189–194 which make up the specificity pocket of α-lytic protease is typical for that of an active proteolytic enzyme (Brayer et al., 1982).

A second example, trypsinogen, has been shown to bind inhibitors such as bovine pancreatic trypsin inhibitor (BPTI) (Bode, 1979) and pancreatic secretory trypsin inhibitor (PSTI) (Bolognesi et al., 1982). Furthermore, X-ray structures of the PSTI- and BPTI–trypsinogen complexes revealed that these active site conformations are identical to that seen for trypsin with the only area of structural difference being at the environment of Asp 194 (477). Specifically, in the trypsinogen–PSTI complex (Bolognesi et al., 1982), the carboxylate of Asp 194 (477) is neutralized by the side chain of Lys 156 (429), but, in the BPTI–trypsinogen complex (Bode, 1979), Asp 194 (477) is not close to any counterion originating from the protein molecule. However, if the dipeptide Ile–Val or Val–Val is added to the BPTI–trypsinogen complex, the α-amino group of the dipeptide interacts with the carboxylate of Asp 194 (477). Thus, these X-ray structures give support to the hypothesis that the zymogen and mutant form of serine proteases may exist in an active conformation even though the carboxylate of Asp 194 (477) is not stabilized by the free α-amino terminus of residue 16 (276).

Although the X-ray structure of t-PA is not known, the high degree of sequence homology between the serine protease domain of t-PA and other serine proteases suggests that the structure of t-PA should be very similar to that of other serine proteases. On the basis of this fact, molecular models of the serine protease domain of sct-PA and tct-PA were constructed. The model of tct-PA was derived from the structure of α-chymotrypsin (Birktoft & Blow, 1972; Blevins & Tulinsky,

Chart I

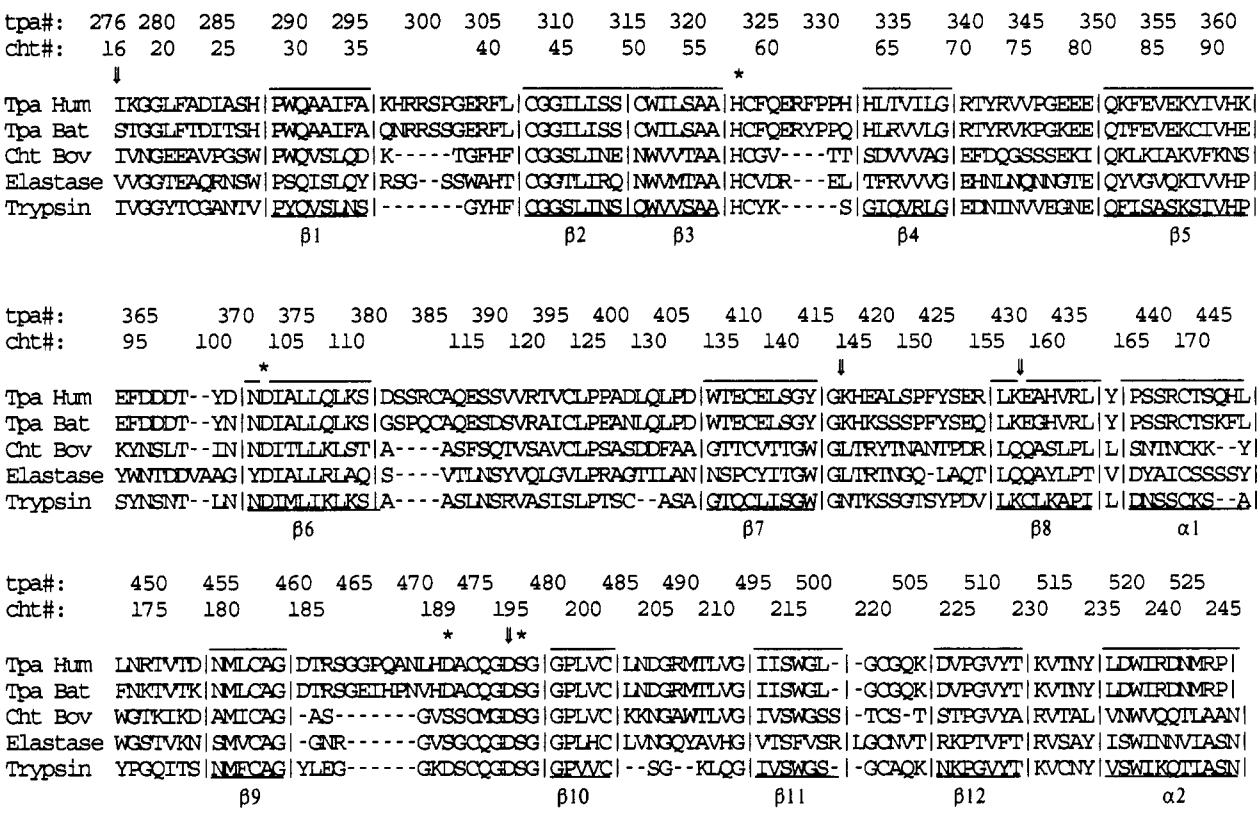

1985). Two different models were developed for sct-PA; the "inactive" zymogen conformation was based on chymotrypsinogen (Birktoft et al., 1976; Wang et al., 1985), while the "active" conformation was based on PSTI–trypsinogen (Bolognesi et al., 1982). According to these models, the only area of structural difference between "active" sct-PA and tct-PA is at the environment of Asp 194 (477), which should not interact with any of the nitroxide spin labels employed in this study.

The model of sct-PA "active" conformation indicated that, as is the case with α-lytic protease and trypsinogen complexed with PSTI, Asp 194 (477) can interact with residues other than the amino-terminal Ile 16 (276). These residues were Lys 156 (429), 143 (416), and 17 (277). Among these Lys 156 (429) appeared to be more favorably oriented for possible interactions with Asp 194 (477), while extensive rearrangement of the main chain at residues 142–144 would be required to bring Lys 143 (416) into contact with Asp 194 (477). It should be noted that both Lys 143 (416) and Lys 156 (477) have been implicated in contributing to the activity of sct-PA by site-directed mutagenesis (Bennett et al., 1991; Petersen et al., 1990). On the other hand, there is no evidence that Lys 17 (277) is critically involved in the activity of sct-PA since site-specific mutagenesis of that residue had no significant influence on the catalytic properties (Petersen et al., 1990; Higgins et al., 1991). This result is further supported by the observation that residue 17 (277) is not a lysine in vampire bat t-PA but instead serine (Gardell et al., 1989). This species occurs only in the one-chain form lacking the ability to be proteolytically cleaved at the normal activation site, i.e., the 15 (275)–16 (276) peptide bond. Importantly, the lysine residues at 143 (416) and 156 (429) are both present in vampire bat t-PA (see Chart I).

In addition to t-PA, a lysine residue is found at position 156 (429) in urokinase, factor X, and trypsinogen, while an arginine residue is seen in rat mast cell protease (Remington et al., 1988) and fiddler crab collagenase (Grant et al., 1987). A lysine is found at position 143 (416) in urokinase, chymotrypsin B, and rat mast cell protease, while an arginine is observed in factor IX and factor X. Among the serine proteases, only in t-PA is a lysine found at position 17 (277), yet it is not observed in all species of t-PA, i.e., bat t-PA (Gardell et al., 1989). It should be emphasized that none of the above proteases has any significant level of activity in their respective zymogen forms. This property is unique to both human and bat t-PA. Another structural feature observed only in t-PA is a large insertion (relative to chymotrypsin and trypsin) which is located between residues 184 (459) and 187 (470). As previously mentioned, this loop was difficult to model and does contain an arginine residue. Thus, this insertion could be another region of importance for the stabilization of the enzymatic active form of sct-PA.

Hence, the above discussion suggests that sct-PA could exist in two conformational states in dynamic equilibrium (Figure 7A): an inactive zymogenic conformation (I) and an active conformation (A). This figure also depicts sct-PA in an "active locked" (AL) conformation that is formed upon binding of substrate or substrate analogues such as the fluorosulfonyl spin labels. In Figure 7B, the interaction of the sulfonyl moiety with the oxyanion hole [formed by the peptide backbone amido groups of Ser 195 (478) and Gly 193 (476)] is also schematically illustrated. The modeling studies presented have shown that Gly 193 (476) undergoes a significant shift in location during the structural transformation from the "inactive" to the "active" conformation (Freer et al., 1970; Birktoft et al., 1976; Bode, 1979). Also recall that stabilization of Asp 194 (477) may be a primary driving force in the formation of an active enzyme that includes the formation of the binding specificity pocket as well as the oxyanion hole. Thus, formation and stabilization of the "active locked" conformation of sct-PA could occur by virtue of the fact that the fluorosulfonyl labels are interacting at and/or assisting in the formation of the oxyanion hole (Kraut, 1977) as well as and

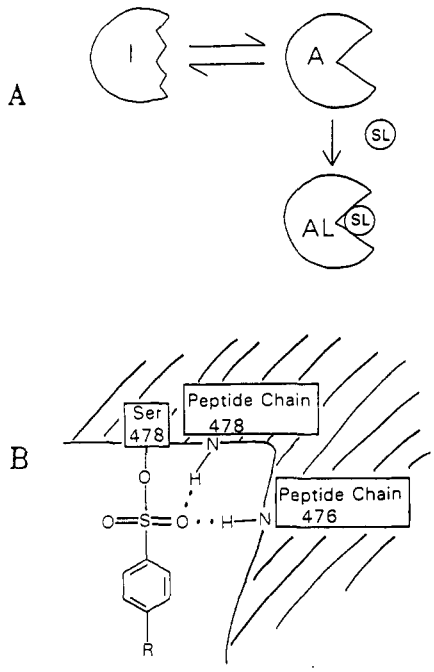

FIGURE 7: (A) Schematic illustration of different proposed conformational states of sct-PA: I is the "inactive", A the "active", and AL the "active locked" conformation. SL represents the nitroxide spin label. (B) Schematic illustration of the interaction of the sulfonyl moiety with the oxyanion hole of sct-PA or tct-PA.

perhaps to a lesser extent by interactions of the binding specificity pocket with the aromatic and hydrophobic moieties of the label.

The results with anthraniloyl-t-PA were unique in that this fluorescent probe was capable of distinguishing between sct-PA and tct-PA. This probe differs from the fluorosulfonyl label, in that it forms a trigonal complex with Ser 195 (478), and this *does not* mimic the tetrahedral transition-state intermediate in the serine protease mechanism. That is, this probe is *not* capable of interacting directly with the oxyanion hole. This has been shown crystallographically for indoleacryloyl-α-chymotrypsin (Henderson, 1970) and for similar acyl probes which are incapable of interacting with the oxyanion hole of γ-chymotrypsin (Stoddard et al., 1990) as well as for trypsin (Mangel et al., 1990). In none of these acyl intermediates is the acyl oxygen interacting with peptide amido groups of Gly 193 (476) and Ser 195 (478). A solvent molecule may perhaps be positioned in the oxyanion hole in this derivative. Thus, these results suggest that in anthraniloyl-t-PA the fluorophore is incapable of stabilizing sct-PA in an "active locked" conformation since it lacks the (strong) stabilizing effects of the tetrahedral transition-state probes.

Finally, in the active site studies, fibrinogen as well as plasmin-degraded fibrinogen fragments were found to have no effect on the ESR or the fluorescence spectra of (tetrahedral transition state) fluorosulfonyl active site labeled sct-PA and tct-PA. On the other hand, fibrinogen binding affected the fluorescence emission of anthraniloyl-R275E-sct-PA but not the corresponding tct-PA derivative. We note that, if tetrahedral active site probes induce a ("fibrin like") conformational shift of sct-PA to an "active" tct-PA-like form, this would render the active site sulfonyl nitroxide (or fluorescent) label insensitive to the binding of fibrin. However, upon binding (341 kDa) fibrinogen, the t-PA/fibrinogen complex should be significantly altered in macromolecular tumbling rate, thereby altering the apparent tumbling motion of the nitroxide spin label on the protease domain of t-PA, reflected as an increase in the $2T_{\parallel}$ of the ESR spectrum. No ESR spectral effects were observed. The most plausible explanations are that, under the conditions of the experiments, the t-PA did not bind fibrinogen or fragments (which is difficult to rationalize with the changes seen in anthraniloyl-t-PA) or, more likely, that the protease and fibrinogen binding domain are conformationally flexible and/or are capable of tumbling independently from one another. As precedence, similar results have been observed by NMR for urokinase and plasminogen which have similar multidomain structures (Bogusky et al., 1989; Oswald et al., 1989; Teuten et al., 1991). Also, the observation that fibrinogen binding altered the fluorescence emission of anthraniloyl-sct-PA, but not anthraniloyl-tct-PA, indicates that binding of fibrinogen to sct-PA induces a conformational change at the active site which does not occur with tct-PA (assuming that the extent of fibrinogen binding was comparable in both experiments). Furthermore, the fluorescence change was in the same direction as that observed during the sct-PA to tct-PA conversion (quenching of fluorescence), which might also suggest that this change was consistent with a conformational shift from "inactive" to "active" sct-PA as discussed above for the putative sct-PA models.

In conclusion, the mechanism for sct-PA activity could be due to an equilibrium between an active and zymogenic conformation centering around the binding specificity pocket. Upon substrate binding, the conformational equilibrium of sct-PA (see Figure 6A) is shifted further toward the active enzyme conformation, either by substrate binding to both conformational forms and inducing a conformational transition of the zymogen or by a preferential binding to the active conformation of sct-PA. This equilibrium could be similar to that proposed to occur for trypsinogen/PSTI-trypsinogen (Bode, 1979; Bolognesi et al., 1982). However, it is most likely that sct-PA is considerably more flexible than trypsinogen such that the equilibrium between the inactive and active forms lies much closer to unity. While trypsinogen is capable of undergoing the above conformational shift, it possess only a small fraction of the activity (ca 10^{-7} to 10^{-8}) of its two-chain counterpart, trypsin. This is to be compared with the ca. 3–6-fold difference in activity between sct-PA and tct-PA. Also, as discussed above, other serine proteases which possess lysine/arginine residues at positions 143 (416) and 156 (429) do not exhibit the unique activity of sct-PA. Thus, while the stabilization of Asp 194 (477) by lysines 277, 416, and 429 in sct-PA, as well as in the presence of a transition-state analogue such as the sulfonyl labels in this study may assist in the "activation" of sct-PA, the unique activity most likely has its basis in a more complicated intrinsic property of the protein.

Registry No. t-PA, 139639-23-9; Ser, 56-45-1.

REFERENCES

Bajaj, S. P., Spitzer, S. G., Welsh, W. J., Kasper, C. K., & Birktoft, J. J. (1990) *J. Biol. Chem. 265*, 2956–2961.

Bennett, W. F., Paoni, N. F., Keyt, B. A., Botstein, D., Jones, A. J. S., Presta, L., Wurm, F., & Zoller, M. J. (1991) *J. Biol. Chem. 265*, 5191–5201.

Berliner, L. J., & Wong, S. S. (1974) *J. Biol. Chem. 249*, 1668–1677.

Berliner, L. J., & Shen, Y. Y. L. (1977a) *Biochemistry 16*, 4622–4626.

Berliner, L. J., & Shen, Y. Y. L. (1977b) *Thromb. Res. 12*, 15–25.

Berliner, L. J., Bauer, R. S., Chang, T. L., Fenton, J. W., II, & Shen, Y. Y. L. (1981) *Biochemistry 20*, 1831–1837.

Berliner, L. J., Birktoft, J. J., Miller, T. L., Musci, G, Scheffler, J. E., Shen, Y. Y., & Sugawara, Y. (1987) *Ann. N.Y. Acad. Sci. 485*, 80–95.
Bernstein, F. C., Koetzle, T. F., Williams, G. J. B., Meyer, E. F., Jr., Brice, M. D., Rodgers, J. R., Kennard, O., Shimanouchi, T., & Tasumi, M. (1977) *J. Mol. Biol. 112*, 535–542.
Birktoft, J. J., & Blow, D. M. (1972) *J. Mol. Biol. 68*, 187.
Birktoft, J. J., Kraut, J., & Freer, S. J. (1976) *Biochemistry 15*, 4481–4485.
Blevins, R. A., & Tulinsky, A. (1985) *J. Biol. Chem. 260*, 4264–4275; 8865–8872.
Bode, W. (1979) *J. Mol. Biol. 127*, 357–374.
Bode, W., Fehlhammer, H., & Huber, R. (1976) *J. Mol. Biol. 106*, 325–335.
Bode, W., Schwager, P., & Huber, R. (1978) *J. Mol. Biol. 118*, 99–112.
Bogusky, M. J., Dobson, C. A., & Smith, R. A. G. (1989) *Biochemistry 28*, 6728–6735.
Bolognesi, M., Gatti, G., Menegatti, E., Guarneri, M., Marquart, M., Papamokos, E., & Huber, R. (1982) *J. Mol. Biol. 162*, 839.
Boose, J. A., Kuismanen, E., Gerard, R., Sambrook, J., & Gething, M. J. (1989) *Biochemistry 28*, 635–543.
Brayer, G. D., Delbaere, L. T. J., & James, M. N. G. (1979) *J. Mol. Biol. 131*, 743–775.
Brünger, A. T. (1988) *J. Mol. Biol. 203*, 803–816.
Cambillau, C., & Horjales, E. (1987) *J. Mol. Graphics 5*, 174–177.
Chen, Z., & Bode, W. (1983) *J. Mol. Biol. 164*, 283.
Craik, C. S., Rutter, W. J., & Fletterick, R. (1983) *Science 220*, 1125–1129.
Devereux, J., Haerberli, P., & Smithies, O. (1984) *Nucleic Acids Res. 12*, 387.
Freer, S. T., Kraut, J. D., Wright, H. T., & Xuong, N. H. (1970) *Biochemistry 9*, 1997–2009.
Fujinaga, M., & James, M. N. G. (1987) *J. Mol. Biol. 195*, 373.
Gardell, S. J., Duong, L. T., Diehl, R. E., York, J. D., Hare, T. R., Register, R. B., Jacobs, J. W., & Dixon, R. A. T. (1989) *J. Biol. Chem. 264*, 17947–17952.
Grant, G. A., Eisen, A. Z., Marmer, B. L., Roswit, W. T., & Goldberg, G. I. (1987) *J. Biol. Chem. 262*, 5886–5889.
Hartley, B. S. (1970) *Philos. Trans. R. Soc. London B 257*, 67–77.
Henderson, R. (1976) *J. Mol. Biol. 54*, 341–354.
Higgins, D. L., & Lamb, C. M. (1986) *Arch. Biochem. Biophys. 249*, 418–426.
Higgins, D. L., & Vehar, G. A. (1987) *Biochemistry 26*, 7786–7791.
Higgins, D. L., Young, S. L., & Wong, A. (1991) *Fibrinolysis 5*, 43.
Huber, R., & Bode, W. (1978) *Acc. Chem. Res. 11*, 114.
Jones, M. O., & Stroud, R. M. (1986) *Protein Data Bank* entry 2TGD, Brookhaven National Laboratory, Upton, NY.
Jones, T. A., & Thirup, S. (1986) *Eur. J. Biochem. 5*, 819–822.
Kerr, M. A., Walsh, K. A., & Neurath, H. (1975) *Biochemistry 14*, 5088–5094.
Kimmel, R. (1987) M.S. Thesis, Washington University, St. Louis, MO.
Kraut, J. (1977) *Annu. Rev. Biochem. 46*, 331–358.
Loscalzo, J. (1988) *J. Clin. Invest. 82*, 1391–1397.
Mangel, W. F., Singer, P. T., Cyr, D. M., Umland, T. C., Toledo, D. L., Stroud, R. M., Pflugrath, J. W., & Sweet, R. M. (1990) *Biochemistry 29*, 8351–8357.
Musci, G., Berliner, L. J., & Esmon, C. T. (1988) *Biochemistry 27*, 769–773.
Navia, M. A., McKeever, B. M., Springer, J. P., Lin, T., Williams, H. R., Fluder, E. M., Dorn, C. P., & Hoogsteen, K. (1989) *Proc. Natl. Acad. Sci. U.S.A. 86*, 7–11.
Nienaber, V. L., & Berliner, L. J. (1991) *Thromb. Haemostasis 65*, 40–45.
Oswald, R. E., Bogusky, M. J., Bamberger, M., Smith, R. A. G., & Dobson, C. A. (1989) *Nature 337*, 579–582.
Petersen, L. C., Johannessen, M., Foster, D., Kumar, A., & Mulvihill, E. (1988) *Biochim. Biophys. Acta 952*, 245–254.
Petersen, L. C., Boel, E., Johannessen, M., & Foster, D. (1990) *Biochemistry 29*, 3451–3457.
Remington, S. J., Woodbury, R. G., Reynolds, R. A., Matthews, B. W., & Neurath, H. (1988) *Biochemistry 27*, 8097.
Sawyer, L., Shotton, D. M., Campbell, J. W., Wendell, P. L., Muirhead, H., & Watson, H. C. (1978) *J. Mol. Biol. 118*, 137–208.
Stoddard, B. L., Bruhnke, J., Koenigs, P., Porter, P., Ringe, D., & Petsko, G. (1990) *Biochemistry 29*, 4871–4879; 8042–8051.
Stroud, R., Kay, L., & Dickerson, R. (1974) *J. Mol. Biol. 83*, 185–208.
Sugawara, Y., Birktoft, J. J., & Berliner, L. J. (1986) *Semin. Thromb. Hemostasis 12*, 209–212.
Tate, K. M., Higgins, D. L., Holmes, W. E., Winkler, M. E., Heyneker, H. L., & Vehar, G. A. (1987) *Biochemistry 26*, 338–343.
Teuten, A. J., Smith, R. A. G., & Dobson, C. A. (1991) *FEBS Lett. 278*, 17–22.
Urano, T., DeSerrano, V. S., Urano, S., & Castellino, F. J. (1989) *Arch. Biochem. Biophys. 270*, 356–363.
Vaz, W. L. C., & Schoellmann, G. (1976) *Biochim. Biophys. Acta 439*, 194–218.
Wang, D., Bode, W., & Huber, R. (1985) *J. Mol. Biol. 185*, 595.
Wong, S. S., Quiggle, K., Triplett, C., & Berliner, L. J. (1974) *J. Biol. Chem. 249*, 1678–1682.